引用格式：WANG Yunxin, ZHU Jianglei, ZHAO Jie, et al. Continuous Terahertz Image-plane Digital Holography Based on TPX Lens[J]. Acta Photonica Sinica, 2022, 51(4):0409001
王云新,朱江磊,赵洁,等.基于TPX透镜的连续太赫兹波像面数字全息成像研究[J].光子学报,2022,51(4):0409001

基于TPX透镜的连续太赫兹波像面数字全息成像研究

王云新[1,2],朱江磊[1,2],赵洁[1,2],王大勇[1,2],戎路[1,2],林述锋[1,2]
(1 北京工业大学 理学部 物理与光电学院,北京 100124)
(2 北京市精密测控技术与仪器工程技术研究中心,北京 100124)

摘 要:太赫兹波对非极性材料具有良好的穿透性,与太赫兹波强度成像相比,相衬成像能够更好的反映物体的内部结构。本文提出了基于TPX透镜的连续太赫兹波像面数字全息相衬成像方法,研究了全息记录和再现过程,利用曲面拟合畸变校正去除TPX透镜引入的二次相位畸变。实验搭建了太赫兹波像面数字全息成像系统,利用振幅型西门子星样品对系统的成像分辨率进行了定量分析,同时对有机材料和生物样品两种相位型样品进行成像,实验验证了该相衬成像方法的有效性。在太赫兹波段引入像面成像,有利于提高太赫兹成像分辨率及成像质量,在生物医学成像、无损检测等领域具有广泛的应用前景。

关键词:太赫兹成像;数字全息;离轴数字全息;像面数字全息;畸变校正
中图分类号:O438.2 **文献标识码**:A **doi**:10.3788/gzxb20225104.0409001

0 引言

太赫兹(Terahertz, THz)波介于红外波与微波之间,具备穿透性、强水吸收、低光子能量等特点,在生物医学成像[1-3]、反恐安检[4-5]和无损检测[6-7]等相关领域均有着广泛应用。太赫兹波良好的穿透性有利于检测物体的内部结构,与单纯的太赫兹波强度成像相比,相衬成像能够更好的反映物体的内部结构。连续太赫兹波相衬成像可分为单点探测器逐点扫描采集方式和面阵探测器全场记录方式,前者数据采集速率较低,无法对大尺寸样品进行快速成像[8];后者数据采集速率快,但也对探测器的像素尺寸和动态范围提出了更高的要求。连续太赫兹波数字全息成像是利用面阵式探测器全场记录全息图,再通过重建算法获得样品的复振幅信息。根据光路结构不同,连续太赫兹波数字全息成像可分为同轴数字全息成像[9-10]和离轴数字全息成像[11-13]。前者可充分利用探测器的空间带宽积,但对样品有一定的要求,需要通过样品后的直透光和衍射光能量比足够高,同时存在孪生像干扰问题;后者在物光和参考光之间引入一定角度,解决了孪生像问题,重建过程简单,更易于实时成像。

与离轴菲涅耳数字全息成像相比,离轴像面数字全息利用显微物镜直接采集物体的成像信息,再现过程简单[14-15],具有计算速度快、分辨率高等优势,广泛应用于可见光波段相衬成像中,且已与其它高分辨成像技术结合,衍生出了多角度照明数字全息、结构光照明数字全息等成像技术[16-19]。但在太赫兹波段,由于太赫兹器件的匮乏和极性物质对太赫兹的强吸收,导致太赫兹全场相衬成像通常要求光路结构紧凑简单,目前尚未见太赫兹像面数字全息成像的相关报道。近些年,激光器[20]、探测器[21]、光栅[22]等各种太赫兹器件得到快速发展,涌现出了大数值孔径太赫兹透镜[23]、太赫兹固体浸没物镜[24]等新型太赫兹成像元件,为太赫兹

基金项目:国家自然科学基金(Nos. 62075001,62175004),北京市教委科技重点项目(No. KZ202010005008)
第一作者:王云新(1981—),女,副教授,博士,主要研究方向为光学信息处理、数字全息成像及微波光子学。Email: yxwang@ bjut.edu.cn
通讯作者:赵洁(1982—),女,讲师,博士,主要研究方向为光信息处理、光学成像及数字全息术。Email: zhaojie@bjut.edu.cn
收稿日期:2021-12-12;**录用日期**:2022-02-23

成像的发展提供了有力的硬件支撑。

本文提出一种基于TPX透镜的连续太赫兹波像面数字全息成像方法，在保证系统结构相对简单紧凑的情况下，通过在离轴数字全息光路中加入TPX透镜成像，搭建了像面数字全息成像光路，针对透镜带来的相位畸变，使用曲面拟合的方法进行校正，提高了连续太赫兹波像面数字全息成像的重建像质量，分别对振幅型和相位型样品进行了成像实验，分析了系统的成像分辨率，并实验验证了该相衬成像方法的有效性。

1 像面数字全息理论

连续太赫兹波像面数字全息成像原理如图1所示，一束单色太赫兹平面波垂直照射物体，设物体的复振幅分布为$U_o(x_o, y_o)$，其衍射传播距离d_o后到达透镜前表面，经透镜的二次位相调制，再衍射传播距离d_i后到达透镜的像平面，傍轴近似条件下像平面的光场复振幅分布$U_i(x_i, y_i)$可表示为[25]

$$U_i(x_i, y_i)=U_o\left(-\frac{x_i}{M}, -\frac{y_i}{M}\right)\exp\left[\frac{jk}{2}\left(\frac{d_o+d_i}{d_i^2}\right)\left(x_i^{\,2}+y_i^{\,2}\right)\right] \tag{1}$$

式中，$M=\frac{d_i}{d_o}$是成像系统的放大倍率。可见，像平面光场分布本质是物平面光场分布放大几何像与一个二次位相因子的乘积。

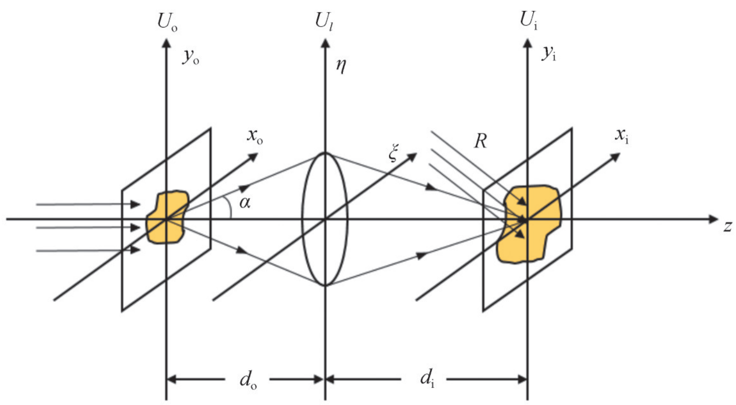

图1 像面数字全息成像原理

Fig. 1 The principle diagram of image-plane digital holography

在像面数字全息系统中的像面上，一束倾斜平面波$R(x_i, y_i)$作为参考与像$U_i(x_i, y_i)$干涉，$R(x_i, y_i)$可表示为

$$R(x_i, y_i)=\exp\left[-j2\pi\left(\frac{\cos\alpha}{\lambda}x_i+\frac{\cos\beta}{\lambda}y_i\right)\right] \tag{2}$$

式中，$\frac{\cos\alpha}{\lambda}$、$\frac{\cos\beta}{\lambda}$分别是参考光的方向余弦。则全息图的强度分布可表示为

$$I(x_i, y_i)=\left|U_i\right|^2+\left|R\right|^2+U_i^{\,*}R+U_iR^* \tag{3}$$

物信息包含在全息图的U_iR^*项中，表达式为

$$U_iR^*=U_o\left(-\frac{x_i}{M}, -\frac{y_i}{M}\right)\exp\left[\frac{jk}{2}\left(\frac{d_o+d_i}{d_i^2}\right)\left(x_i^{\,2}+y_i^{\,2}\right)\right]\exp\left[-j2\pi\left(\frac{\cos\alpha}{\lambda}x_i+\frac{\cos\beta}{\lambda}y_i\right)\right] \tag{4}$$

传统的频谱滤波法只能滤除参考光带来的一次相位畸变。为此利用曲面拟合法进一步消除二次相位畸变。重建的相位结果$\phi(x_i, y_i)$可表示为

$$\phi(x_i, y_i)=\phi_0(x_i, y_i)+\phi_a(x_i, y_i) \tag{5}$$

式中，$\phi_0(x_i, y_i)$是待测物体的相位信息，$\phi_a(x_i, y_i)$是相位畸变。利用泽尼克多项式近似计算二次相位畸变$\phi_a'(x_i, y_i)$，可表示为[24]

$$\phi_a'(x_i, y_i) = a_1 x_i^2 y_i^2 + a_2 x_i^2 y_i + a_3 x_i y_i^2 + a_4 x_i^2 + a_5 y_i^2 + a_6 x_i y_i + a_7 x_i + a_8 y_i + a_9 \tag{6}$$

$a_1 \sim a_9$是拟合的参数，可由式(7)得到。

$$\boldsymbol{A}_{3\times3} = \begin{pmatrix} a_9 & a_8 & a_5 \\ a_7 & a_6 & a_3 \\ a_4 & a_2 & a_1 \end{pmatrix} = (\boldsymbol{B}^{\mathrm{T}}\boldsymbol{B})^{-1}\boldsymbol{B}^{\mathrm{T}}\phi\boldsymbol{G}(\boldsymbol{G}^{\mathrm{T}}\boldsymbol{G})^{-1} \tag{7}$$

其中，$B_{t\times3}$和$G_{t\times3}$定义为

$$\boldsymbol{B}_{t\times3} \text{ or } \boldsymbol{G}_{t\times3} = \begin{pmatrix} 1 & 1 & 1 \\ 1 & 2 & 4 \\ \vdots & \vdots & \vdots \\ 1 & t & t^2 \end{pmatrix} \tag{8}$$

式中，t是图像矩阵的行数，图像矩阵需为方矩阵。

若光学成像系统的有效数值孔径为NA，则理论上其横向分辨率$\delta_{\min}$可以表示为[26]

$$\delta_{\min} = \frac{0.82\lambda}{\mathrm{NA}} \tag{9}$$

2　实验装置

由于太赫兹离轴数字全息要求较大的离轴夹角，因此根据图1搭建了基于三角式马赫泽德干涉光路的连续太赫兹波像面数字全息成像系统，实验装置如图2所示。连续太赫兹源是二氧化碳激光泵浦的远红外气体激光器(295-FIRL-HP; Edinburgh Instruments Ltd., UK)，其中心波长是118.83 μm(对应中心频率为2.52 THz)，最大输出功率为500 mW。激光器出射光斑直径约为11 mm，经两个镀金离轴抛物面镜(PM1，焦距为50.8 mm；PM2，焦距为152.4 mm)扩束准直为直径约为33 mm的平行光，然后经过高阻硅分光棱镜(BS)分为物光和参考光。物光路采用TPX(4-甲基戊烯聚合物)透镜，其直径为50.8 mm，焦距为50 mm，物体与探测器靶面的位置满足物像关系，实验中物距为75 mm，像距为150 mm，系统的成像放大倍率约为2倍。透镜所成的像与经过镀金反射镜(M)反射的参考光干涉形成全息图，利用热释电探测器(Pyrocam IV，像素数为320×320，像素尺寸为80 μm×80 μm)记录全息图。为了增强干涉条纹的对比度，在50 Hz斩波频率下记录500帧干涉图，并通过高斯拟合累加获得最终的全息图。

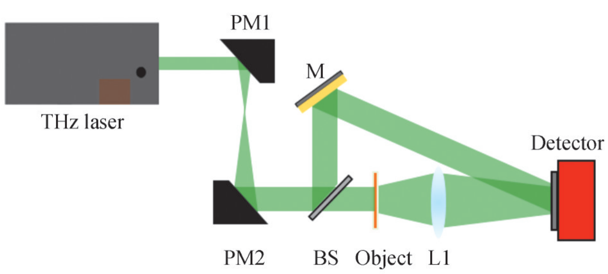

图2　连续太赫兹波像面数字全息成像实验装置图

Fig.2　Schematic of the experimental configuration of continuous-wave terahertz image-plane digital holography

3　结果与分析

为了验证系统的成像分辨率，使用如图3(a)所示的振幅型二值样品作为待测样品，该样品是在硅片上用光刻法镀金的西门子星，图案直径为20 mm，硅片厚度为500 μm，镀金层厚度为50 nm。图3(b)是拍摄的离轴像面全息图，由于透镜会引入二次相位畸变，因此全息图中的干涉条纹并非是直条纹。图3(c)是全息图的频谱，+1级谱用红色圆圈标记。像面数字全息中，将该+1级谱移至频谱图中心，去除参考光引入的一次相位畸变，可获得物体的频谱信息，再对其做傅里叶逆变换，即可得到物体的复振幅分布。图3(d)是重建的振幅结果，像的半径占据247个像素，其对应实际物理尺寸为19.8 mm，因此系统的实际放大倍率为1.98，根据物像距关系算得系统的理论放大倍率为2，两者较为吻合。同时由于系统放大倍率为1.98，像的尺寸远远大于探测器靶面，因此探测器只能采集到西门子星样品的四分之一图像。由于所用样品是扇形西门子

星，所以可将重建结果中距西门子星中心最近的可分辨相邻扇形条的距离作为成像分辨率。图3(d)中的红色虚线即为重建振幅像中可分辨的最小区域，其对应的横向分辨率为327 μm。TPX透镜的数值孔径由物距和透镜直径共同决定，经计算其数值孔径为0.32，结合式(9)可得实验系统的理论分辨率为304 μm，可见实际分辨率与理论分辨率较为接近。图3(e)是曲面拟合前重建的相位像，由式(1)可知，重建的相位像中包含了二次相位畸变，可以从图3(e)中看到待测物体信息完全淹没在严重的二次相位畸变中。曲面拟合校正后得到去除畸变的相位像如图3(f)所示，可以清晰看到物体的细节信息。由于西门子星样品是二值型样品，因此不透区域为随机相位，透过区域的相位应为均匀分布。图3(f)中黄色方框位于物体的透光区域，其均方差为1.38×10^{-13} rad，可见成像区域较为平坦，实验结果表明本系统很好的去除了相位畸变，获得较好的振幅和相位像。

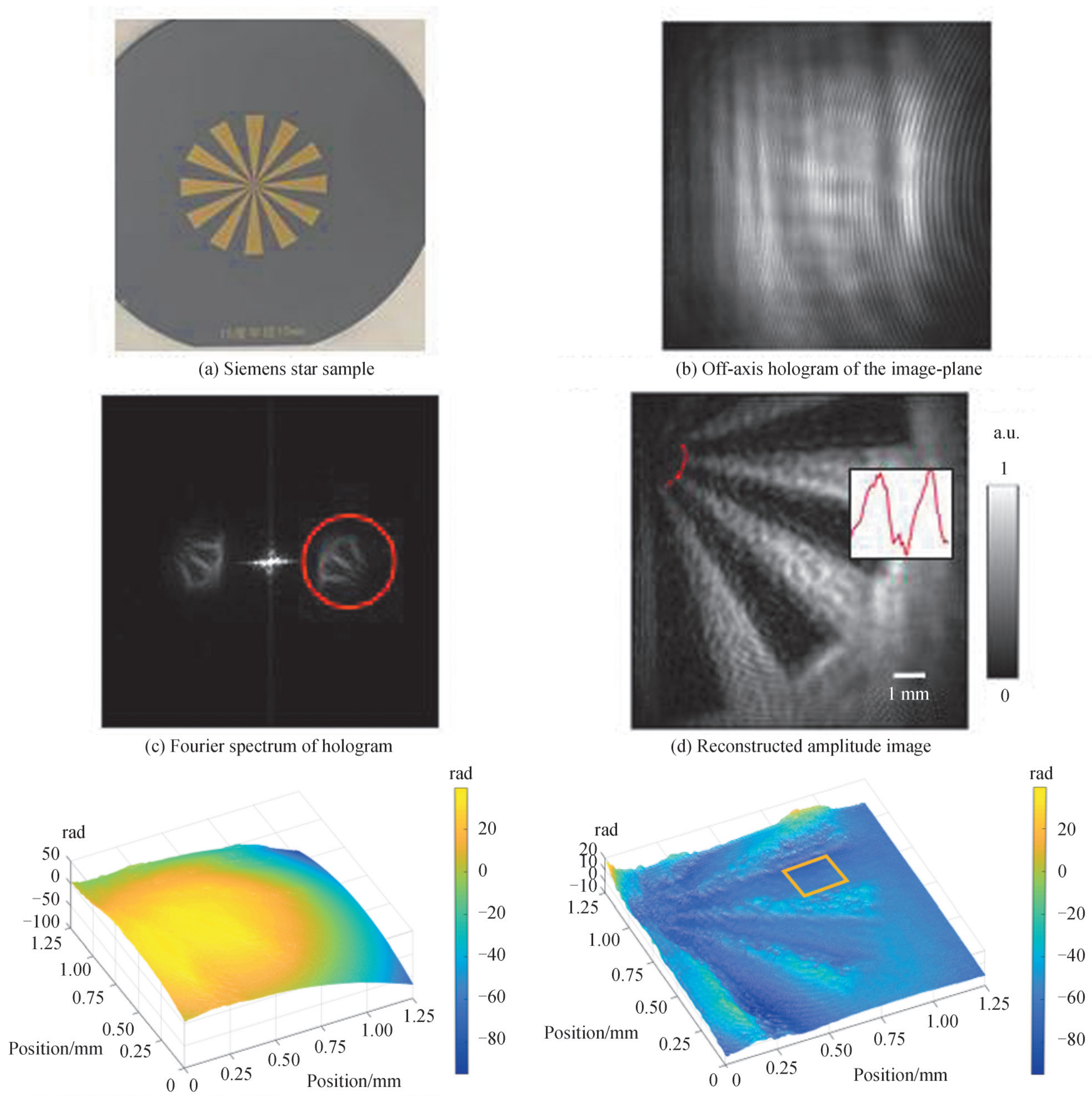

(a) Siemens star sample
(b) Off-axis hologram of the image-plane
(c) Fourier spectrum of hologram
(d) Reconstructed amplitude image
(e) Reconstructed phase image before surface fitting aberration correction
(f) Reconstructed phase image after surface fitting aberration correction

图3　太赫兹振幅型样品重建结果

Fig. 3　Reconstruction images of terahertz amplitude type samples

为了验证像面全息相衬成像的有效性,分别对有机材料和生物样品进行了成像实验。如图4(a)为具有一些凸起特征图案的有机材料聚丙烯片(n=1.51@2.52 THz),特征图案与附近平坦区域的相对落差为30 μm。图4(b)是聚丙烯片的像面离轴全息图,整个图案都在全息图的干涉区域内。图4(c)是全息图的频谱,+1级谱用红色圆圈标记,0级与±1级分离。图4(d)和(f)分别是重建的振幅像和相位像,从重建相位中可以明显看到样品的特征轮廓,分别提取部分图(f)中背景区域和图案区域,得到其平均相位差约为0.78 rad,结合折射率计算可得到对应的凸起图案平均高度约为29.0 μm,与实际值较为吻合,相对测量误差为3.4%。

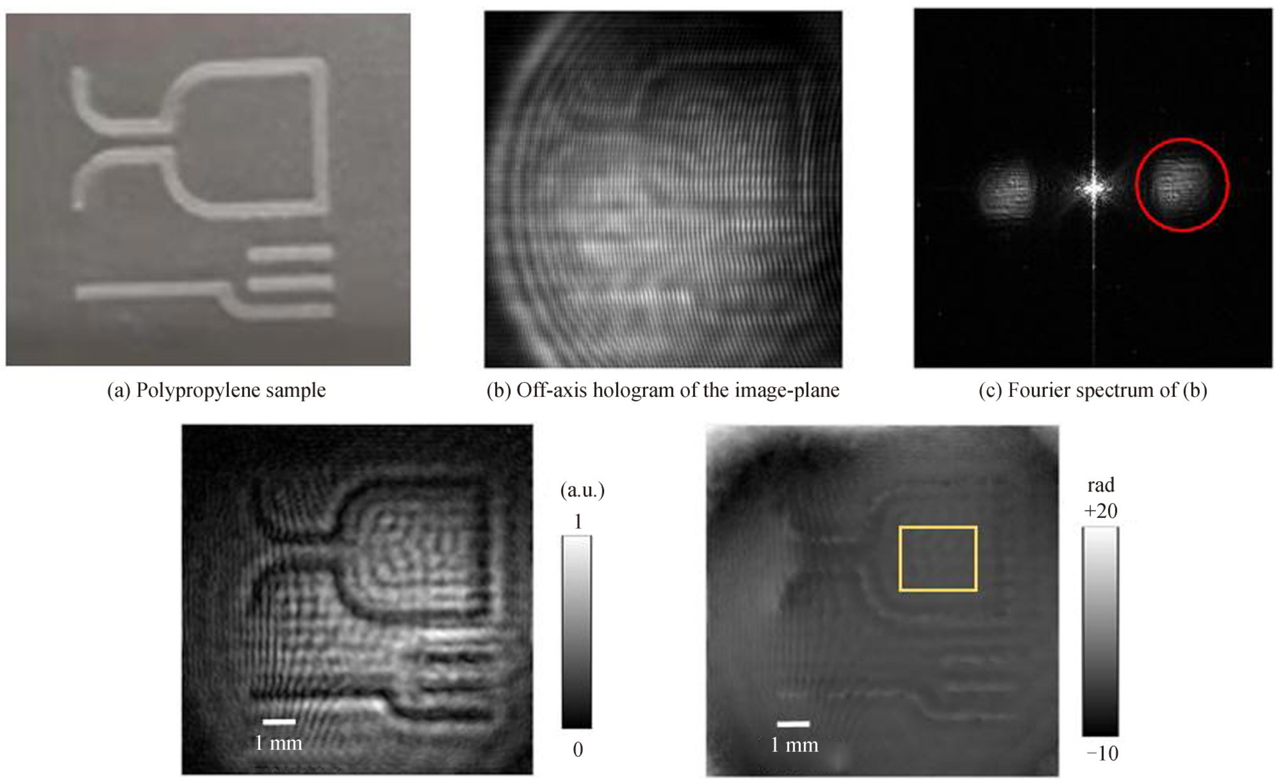

(a) Polypropylene sample (b) Off-axis hologram of the image-plane (c) Fourier spectrum of (b)

(d) Reconstructed amplitude image (e) Reconstructed phase image

图4 太赫兹相位型样品重建结果

Fig 4 Reconstruction results of terahertz phase-type samples

最后,对晒干脱水后的小宝塔水草的生物样品进行成像,样品照片如图5(a)所示,黄色方框区域为成像视场。图5(b)是生物样品的像面离轴数字全息图,图5(c)是其对应的频谱,图5(d)和(e)分别是其重建振幅像和重建相位像。由于水草已经晒干脱水,所以对太赫兹波的吸收很小,因此在图5(d)重建振幅结果中几乎看不见水草,而水草因为具有一定的结构且与空气的折射率不同,因此在图5(f)重建相位结果中就可以更好地分辨水草的结构。以上相位成像结果都证明了太赫兹像面数字全息系统的有效性。

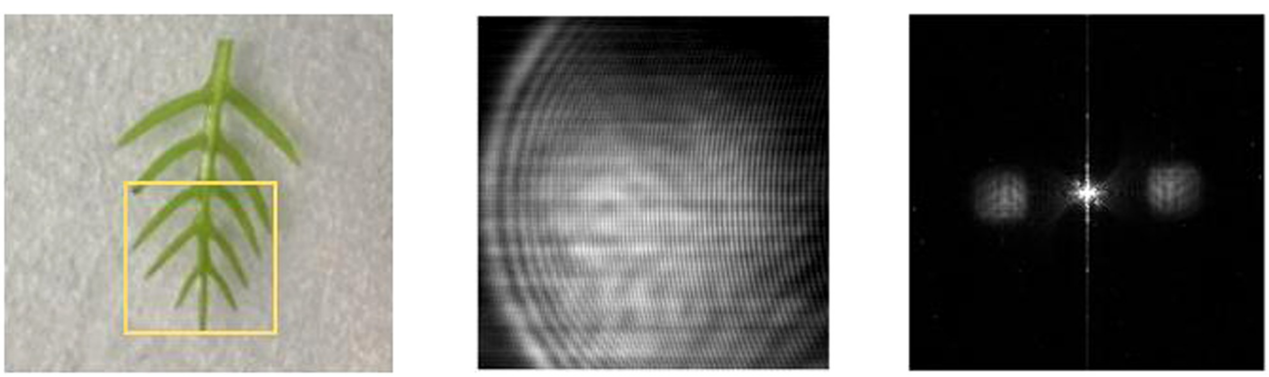

(a) Small pagoda water plant sample (b) Off-axis hologram of the image-plane (c) Fourier spectrum of (b)

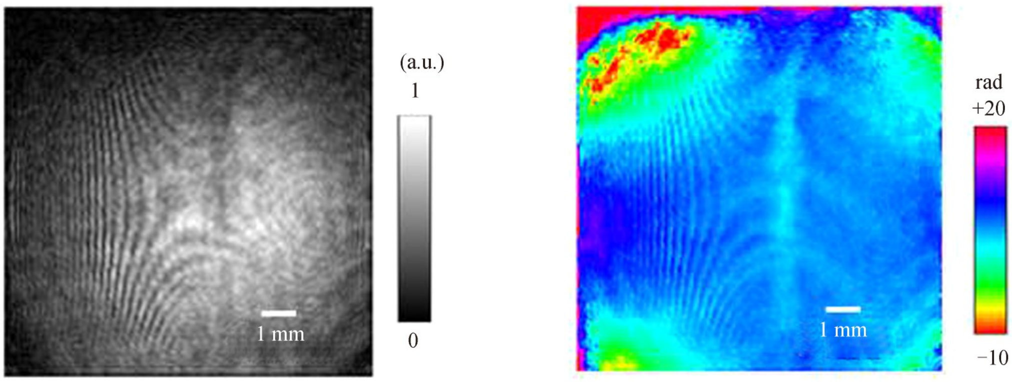

(d) Reconstructed amplitude image　　(e) Reconstructed phase image

图5　太赫兹相位型样品重建结果

Fig. 5　Results of terahertz phase-type sample reconstruction

4　结论

本文研究了基于TPX透镜的连续太赫兹波像面数字全息成像方法，分析了数字全息图的记录和再现过程，并进一步采用基于曲面拟合的畸变校正方法去除透镜引入的二次相位畸变。构建了基于TPX透镜的太赫兹像面数字全息成像系统，利用振幅型西门子星定量分析了系统的成像分辨率，实验结果表明系统分辨率达到327 μm。在此基础上，对有机材料样品和生物样品进行成像，获取了高质量的振幅和相位像，实验验证了太赫兹波像面数字全息成像的有效性。在太赫兹波段引入像面成像，有利于提高太赫兹成像分辨率及成像质量，在生物医学成像、无损检测等领域具有广泛的应用前景。此外，结合最新发展的太赫兹成像器件，有望将其与傅里叶叠层成像、基于光强传输方程成像等新兴技术相结合，进一步促进太赫兹相衬成像的发展。

参考文献

[1] DORADLA P, ALAVI K, JOSEPH C, et al. Detection of colon cancer by continuous-wave terahertz polarization imaging technique[J]. Journal of Biomedical Optics, 2013, 18(9):504.

[2] ZAYTSEV K I, KUDRIN K G, KARASIK V E, et al. In vivo terahertz spectroscopy of pigmentary skin nevi: pilot study of non-invasive early diagnosis of dysplasia[J]. Applied Physics Letters, 2015, 106(5): 53702.

[3] AHI K. A method and system for enhancing the resolution of terahertz imaging[J]. Measurement, 2019, 138: 614-619.

[4] YAKOVLEV E V, ZAYTSEV K I, DOLGANOVA I N, et al. Non-destructive evaluation of polymer composite materials at the manufacturing stage using Terahertz pulsed spectroscopy[J]. IEEE Transactions on Terahertz Science and Technology, 2015, 5(5): 810-816.

[5] KOWALSKI M, KASTEK M, WALCZAKOWSKI M, et al. Passive imaging of concealed objects in terahertz and long-wavelength infrared[J]. Applied Optics, 2015, 54(13): 3826.

[6] YOUSEFI B, SFARRA S, IBARRA CASTANEDO C, et al. Comparative analysis on thermal non-destructive testing imagery applying Candid Covariance-Free Incremental Principal Component Thermography (CCIPCT)[J]. Infrared Physics & Technology, 2017, 85: 163-169.

[7] ZHANG Hai, ROBITAILLE F, GROSSE C U, et al. Optical excitation thermography for twill/plain weaves and stitched fabric dry carbon fibre preform inspection[J]. Composites Part A: Applied Science and Manufacturing, 2018, 107: 282-293.

[8] LÖFFLER T, MAY T, AM WEG C, et al. Continuous-wave terahertz imaging with a hybrid system[J]. Applied Physics Letters, 2007, 90(9): 91111.

[9] RONG Lu, LATYCHEVSKAIA T, CHEN Chunhai, et al. Terahertz in-line digital holography of human hepatocellular carcinoma tissue[J]. Scientific Reports, 2015, 5(1): 8445.

[10] LI Zeyu, ZOU Ruijiao, KONG Weipeng, et al. Terahertz synthetic aperture in-line holography with intensity correction and sparsity autofocusing reconstruction[J]. Photonics Research, 2019, 7(12): 1391.

[11] DING Shenghui, LI Qi, LI Yunda, et al. Continuous-wave terahertz digital holography by use of a pyroelectric array camera[J]. Optics Letters, 2011, 36(11): 1993-1995.

[12] LOCATELLI M, RAVARO M, BARTALINI S, et al. Real-time terahertz digital holography with a quantum cascade laser[J]. Scientific Reports, 2015, 5(1): 13566.

[13] WANG Dayong, ZHANG Yaya, RONG Lu, et al. Continuous-wave terahertz self-referencing digital holography based on Fresnel's mirrors[J]. Optics Letters, 2020, 45(4): 913-916.
[14] FU Yu, SHI Hongjian, MIAO Hong. Vibration measurement of a miniature component by high-speed image-plane digital holographic microscopy[J]. Applied Optics, 2009, 48(11): 1990-1997.
[15] MAHAJAN S, TRIVEDI V, VORA P, et al. Highly stable digital holographic microscope using Sagnac interferometer [J]. Optics Letters, 2015, 40(16): 3743-3746.
[16] LAI Xinji, TU Hanyen, WU Chunghsin, et al. Resolution enhancement of spectrum normalization in synthetic aperture digital holographic microscopy[J]. Applied Optics, 2015, 54(1): A51.
[17] ZHENG Cheng, JIN Di, HE Yanping, et al. High spatial and temporal resolution synthetic aperture phase microscopy[J]. Advanced Photonics, 2020, 2(6): 65002.
[18] ZHENG Juanjuan, GAO Peng, YAO Baoli, et al. Digital holographic microscopy with phase-shift-free structured illumination[J]. Photonics Research (Washington, DC), 2014, 2(3): 87.
[19] LAI Xinji, TU Hanyen, LIN Yuchin, et al. Coded aperture structured illumination digital holographic microscopy for superresolution imaging[J]. Optics Letters, 2018, 43(5): 1143-1146.
[20] KHALATPOUR A, PAULSEN A K, DEIMERT C, et al. High-power portable terahertz laser systems[J]. Nature Photonics, 2021, 15(1):16-20.
[21] ZHANG Ya, WATANABE Y, HOSONO S, et al. Room temperature, very sensitive thermometer using a doubly clamped microelectromechanical beam resonator for bolometer applications[J]. Applied Physics Letters, 2016, 108(16): 163503.
[22] YUAN Yiwu, CHENG Jiecheng, DONG Xipu, et al. Terahertz dual-band polarization control and wavefront shaping over freestanding dielectric binary gratings with high efficiency[J]. Optics and Lasers in Engineering, 2021, 143: 106636.
[23] CHERNOMYRDIN N V, FROLOV M E, LEBEDEV S P, et al. Wide-aperture aspherical lens for high-resolution terahertz imaging[J]. Review of Scientific Instruments, 2017, 88(1): 14703.
[24] CHERNOMYRDIN N V, KUCHERYAVENKO A S, KOLONTAEVA G S, et al. Reflection-mode continuous-wave 0.15λ-resolution terahertz solid immersion microscopy of soft biological tissues[J]. Applied Physics Letters, 2018, 113 (11): 111102.
[25] 张亦卓. 生物样品的数字全息显微相衬成像[D]. 北京:北京工业大学, 2012.
[26] MICÓ V, ZHENG Juanjuan, GARCIA J, et al. Resolution enhancement in quantitative phase microscopy[J]. Advances in Optics and Photonics, 2019, 11(1): 135-214.

Continuous Terahertz Image-plane Digital Holography Based on TPX Lens

WANG Yunxin[1,2], ZHU Jianglei[1,2], ZHAO Jie[1,2], WANG Dayong[1,2], RONG Lu[1,2], LIN Shufeng[1,2]

(1 *College of Physics and Optoelectronics, Faculty of Science, Beijng University of Technology, Beijing* 100124, *China*)

(2 *Beijing Engineering Research Center of Precision Measurement Technology and Instruments, Beijing* 100124, *China*)

Abstract: The wavelength of terahertz wave is between those of infrared wave and microwave, with the characteristics of penetration, strong water absorption, and low photon energy, etc. Terahertz imaging has been are widely used in biomedical imaging, anti-terrorism security and non-destructive testing and other fields. The good penetration of terahertz wave is beneficial to detect the internal structure of objects. Phase-contrast imaging can better reflect the internal structure of objects, compared with simple terahertz intensity imaging. Continuous terahertz wave phase-contrast imaging can be divided into point-by-point scanning acquisition method with a single-point detector and full-field recording method with a surface array detector. The former has a low data acquisition rate and cannot image large samples quickly; the latter has a fast data acquisition rate, but also places higher demands on the detector's pixel size and dynamic range. Continuous terahertz wave digital holographic imaging records the hologram by a faceted detector, and then obtains the complex amplitude information of the sample by a reconstruction algorithm. According to different optical path structures, continuous terahertz wave digital holography can be divided into in-line digital holography and off-axis digital holography. In-line digital holography can make full use of the spatial bandwidth product of the detector, but requires a sufficiently high energy ratio of direct and diffracted light after passing through the sample, as well as the problem of twin image interference. Off-axis digital holography introduces a certain angle between the object light and the reference light, which solves the twin image problem and makes the reconstruction process simple.Off-axis image-plane digital holography uses a microscope objective to directly collect the imaging information of the object. Compared with off-axis Fresnel digital holography, this imaging method has fast computation and high resolution, and has been widely applied at visible wavelengths. Besides, this imaging method has been combined with some other high-resolution imaging techniques, resulting in multi-angle illumination digital holography, structured light illumination digital holography etc. However, due to the lack of terahertz devices and the strong absorption of terahertz by polar substances, the terahertz full-field phase-contrast imaging usually requires a compact and simple optical path structure. To the best of my knowledge, no relevant work on terahertz image-plane digital holography has been reported yet. In recent years, various terahertz devices such as lasers, detectors and gratings have been developed rapidly. New terahertz imaging elements such as large numerical aperture terahertz lenses and terahertz solid immersion objectives have emerged, providing strong hardware support for the development of terahertz imaging. In this paper, a continuous terahertz wave image-plane digital holographic imaging method based on TPX lens is proposed. The holographic recording and reproduction process is studied, and the quadratic phase distortion introduced by TPX lens is removed by surface fitting distortion correction. The digital holographic imaging system of terahertz image plane is built. The imaging resolution of the system is quantitatively analyzed by using an amplitude Siemens star sample. Then two phase samples of organic materials and biological samples are imaged. The experiment verifies the effectiveness of the phase contrast imaging method. The introduction of image plane imaging in terahertz band is conducive to improve the resolution and quality of terahertz imaging. It has a wide application prospect in biomedical imaging, nondestructive testing and other fields.

Key words: Terahertz imaging; Digital holography; Off-axis digital holography; Image-plane digital holography; Aberration correction

OCIS Codes: 040.2235; 110.6795; 110.3010; 090.1995; 100.5088

Foundation item: National Natural Science Foundation of China (Nos. 62075001, 62175004), Science Foundation of Education Commission of Beijing (No. KZ202010005008)